

Structure determination of Ag-Ge-S glasses using neutron diffraction

J. H. Lee and A. P. Owens

Department of Chemistry, University of Cambridge, Lensfield Road, Cambridge CB2 1EW, United Kingdom

A. Pradel

Laboratoire de Physicochimie des Matériaux Solides, Université de Montpellier, 34095 Montpellier Cedex 05, France

A. C. Hannon

ISIS Facility, Rutherford Appleton Laboratory, Chilton, Didcot OX11 0QX, United Kingdom

M. Ribes

Laboratoire de Physicochimie des Matériaux Solides, Université de Montpellier, 34095 Montpellier Cedex 05, France

S. R. Elliott

Department of Chemistry, University of Cambridge, Lensfield Road, Cambridge CB2 1EW, United Kingdom

(Received 22 January 1996; revised manuscript received 1 April 1996)

The structure of the superionic glass system $(\text{Ag}_2\text{S})_x(\text{GeS}_2)_{1-x}$, for three compositions $x=0.3, 0.4, 0.5$, has been studied using neutron diffraction, and isotopic-substitution neutron-diffraction experiments have been performed on three silver isotope-substituted ($^{107}\text{Ag}, ^{\text{nat}}\text{Ag}, ^{109}\text{Ag}$) samples of the composition $(\text{Ag}_2\text{S})_{0.5}(\text{GeS}_2)_{0.5}$. The average short-range orderings of Ge-S, Ag-S, and Ge-Ag correlations were identified in the radial distribution functions for the isotopically substituted system of $(\text{Ag}_2\text{S})_{0.5}(\text{GeS}_2)_{0.5}$. From the first and second differences in the three sets of isotopic-substitution neutron-diffraction data, the other three partial correlations (Ag-Ag, Ge-Ge, and S-S), were also identified. By examining unusually broad peaks in the Ag-Ag correlation function, it was concluded that the Ag-Ag distribution was rather homogeneous. We were also able to obtain further information by combining the first and second difference analyses, resulting in a structural model of a slightly elongated GeS_4 tetrahedron with the local environment of Ag^+ ions being threefold coordination by nonbridging sulphur ions. The medium-range order of the host framework was found to be a chainlike structure of linked corner-sharing GeS_4 tetrahedra. Substantial changes in the first and second peaks in the distinct scattering functions $i(Q)$ were found with composition and also with isotopic substitution. It was possible to explain the trends in the changes of the heights of these peaks in the structure factor by applying the void model for the first sharp diffraction peak. [S0163-1829(96)06230-3]

I. INTRODUCTION

Among the so-called superionic conductors, the $(\text{Ag}_2\text{S})_x(\text{GeS}_2)_{1-x}$ system has attracted a great deal of attention from a practical point of view mainly because of its high ionic conductivity.¹ The composition range for which GeS_2 forms a glass with Ag_2S is appreciable ($x=0-0.55$) and the conductivity increases with Ag_2S concentration.¹ Accordingly, the composition $(\text{Ag}_2\text{S})_{0.55}(\text{GeS}_2)_{0.45}$ exhibits the highest room-temperature dc conductivity of all, $1.35 \times 10^{-3} \Omega^{-1}\text{cm}^{-1}$,¹ which makes this glass one of the best silver cation conductors. This system, unlike its alkali sulphide analogs, is attractive from a practical point of view as it is not hygroscopic.² Moreover, a substantial further increase in conductivity can be achieved by the dissolution of doping salts such as AgI and AgCl .^{1,3}

From a theoretical point of view, the mechanism of ionic conduction has been the subject of intense study, with a number of models being proposed.⁴ Despite several plausible interpretations, however, the ionic-conduction mechanism is not yet fully understood. This is due to difficulties encountered in using structural studies to comprehend the conduction pathway of the mobile ions. It is widely recognized that no single experimental technique is sufficient to determine

the structure of glassy materials. However, there is a particular technique, namely isotopic-substitution neutron diffraction, that enables pair-correlation functions to be resolved in a multicomponent system. This technique relies on the fact that the static structure stays unchanged on replacing the isotopes of atomic species but the neutron-diffraction pattern differs because of the different scattering lengths of the isotopes. Using this characteristic, pair-correlation functions can be separated from the total structure factor.⁵

There has been a substantial amount of work done to investigate the structure of the $(\text{Ag}_2\text{S})_x(\text{GeS}_2)_{1-x}$ system. Early Raman spectroscopy studies provided evidence of terminal Ge-S bonds and Ge-S-Ge bridges.¹ Extensive studies have also been performed by extended x-ray-absorption fine structure (EXAFS) and it has been concluded that the basic framework of this system is composed of GeS_4 tetrahedra⁶ as found in GeS_2 glass. The isotopic-substitution neutron-diffraction technique has been applied to the composition $(\text{Ag}_2\text{S})_{0.5}(\text{GeS}_2)_{0.5}$ by varying the Ag isotopes; a preliminary account of this work appeared in Ref. 7.

II. NEUTRON DIFFRACTION

The measured distinct scattering function $i(Q)$ can be directly transformed to several real-space functions such as the

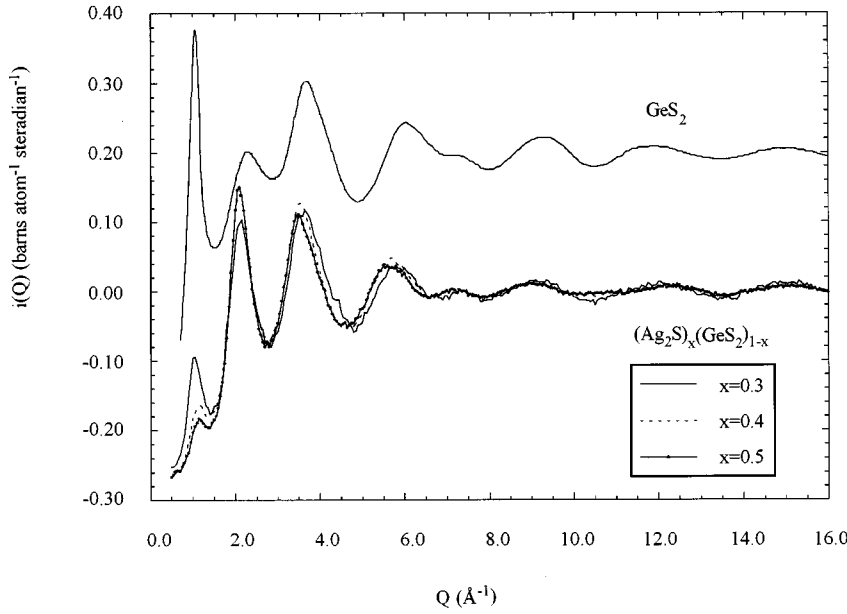


FIG. 1. The distinct scattering functions, $i(Q)$, for the three different compositions of Ag-Ge-S glasses, together with $i(Q)$ for GeS_2 (Ref. 8). The function $i(Q)$ for GeS_2 is displaced by $0.2 \text{ barns atom}^{-1} \text{ Sr}^{-1}$.

differential correlation function $D(r)$, the reduced radial distribution function $G(r)$, and the total correlation function $T(r)$:

$$D(r) = \langle b \rangle^2 G(r) = T(r) - T_0 = \frac{2}{\pi} \int_0^\infty Q i(Q) \sin Qr dQ, \quad (1)$$

where $T_0 = 4\pi\rho^0\langle b \rangle^2$ and ρ^0 is the average density. In multicomponent systems, $\langle b \rangle = \sum_{i=1}^n x_i b_i$, where x_i and b_i are the concentration and scattering length of atomic species i , respectively. In addition, $G(r)$ is a sum of the weighted partial radial distribution functions $G_{ij}(r)$:

$$G(r) = \sum_{ij} w_{ij} G_{ij}(r), \quad (2)$$

where the weighting factor $w_{ij} = x_i x_j b_i b_j / \langle b \rangle^2$ and $T(r)$ is a sum of the partial correlation functions $T_{ij}(r)$:

$$T(r) = \sum_{ij} x_i x_j b_i b_j T_{ij}(r). \quad (3)$$

Among these real-space functions, $D(r)$ is useful for isotopic-substitution analyses and $T(r)$ has the advantage of being convenient for observing symmetries and broadenings of peaks. Moreover, integration of the area under peaks in $rT(r)$ gives the coordination number.

III. EXPERIMENTAL

A. Sample preparation

Three compositions of $(\text{Ag}_2\text{S})_x(\text{GeS}_2)_{1-x}$ glasses ($x=0.3, 0.4$, and 0.5) were prepared by reacting Ag_2S and GeS_2 using the same procedure as reported previously.¹ Isotopically substituted (^{107}Ag , $^{\text{nat}}\text{Ag}$, ^{109}Ag) samples of $(\text{Ag}_2\text{S})_{0.5}(\text{GeS}_2)_{0.5}$ glass were prepared by reacting elemen-

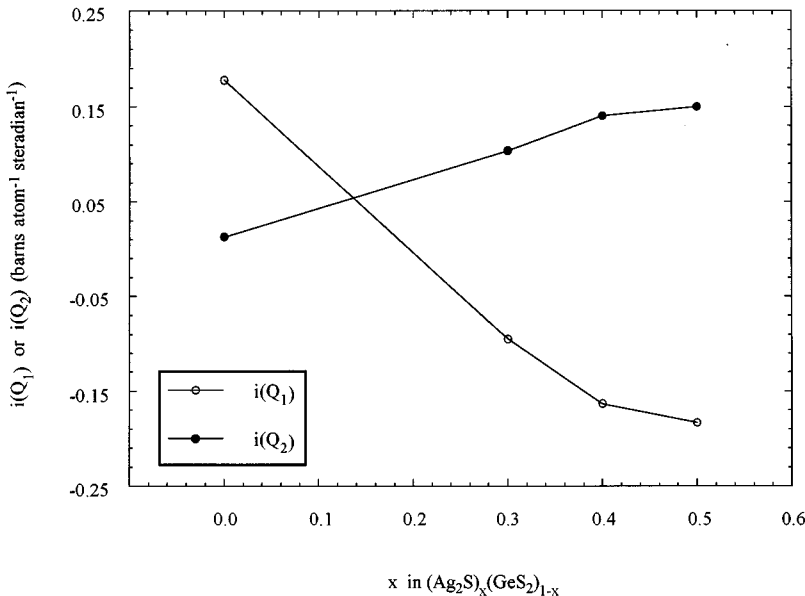


FIG. 2. The variation of the height of the first and second peaks in $i(Q)$, $i(Q_1)$, and $i(Q_2)$, respectively, with Ag_2S composition x in $(\text{Ag}_2\text{S})_x(\text{GeS}_2)_{1-x}$.

TABLE I. Value of $\langle b \rangle^2$ in each sample composition.

	GeS ₂	(Ag ₂ S) _{0.3} (GeS ₂) _{0.7}	(Ag ₂ S) _{0.4} (GeS ₂) _{0.6}	(Ag ₂ S) _{0.5} (GeS ₂) _{0.5}
$\langle b \rangle^2$ (barns)	0.2140	0.2216	0.2242	0.2267

tal Ag and S together with GeS₂. This stoichiometric mixture was placed in a silica tube sealed under vacuum and heated slowly at a rate of 6 K/h up to 900 °C in order to avoid a buildup of pressure due to sulphur vapor. The melt was maintained at this temperature for 2 h and quenched into water.

B. Neutron diffraction

Neutron-diffraction experiments were performed at room temperature on powdered (Ag₂S)_x(GeS₂)_{1-x} ($x=0.3, 0.4,$ and 0.5) glasses using the D4b two-axis diffractometer at the high-flux reactor at the Institut Laue Langevin, Grenoble, France. The maximum value of momentum transfer, Q_{\max} , available in this experiment was approximately 16 \AA^{-1} ($\lambda=0.5 \text{ \AA}$).

Time-of-flight neutron-diffraction experiments were performed at room temperature on powdered isotopically substituted samples of (Ag₂S)_{0.5}(GeS₂)_{0.5} glass using the liquid and amorphous diffractometer (LAD) at the neutron spallation source ISIS, Rutherford Appleton Laboratory, for which Q_{\max} is $30\text{--}50 \text{ \AA}^{-1}$.

IV. RESULTS AND DISCUSSION

A. (Ag₂S)_x(GeS₂)_{1-x} glasses: distinct scattering function $i(Q)$

Figure 1 shows the distinct scattering functions, $i(Q)$, for the three different compositions of Ag-Ge-S, together with $i(Q)$ for GeS₂ (Ref. 8) for comparison. The general features of the three $i(Q)$ functions for the Ag-Ge-S glasses are fairly similar but pronounced differences are observed in the first

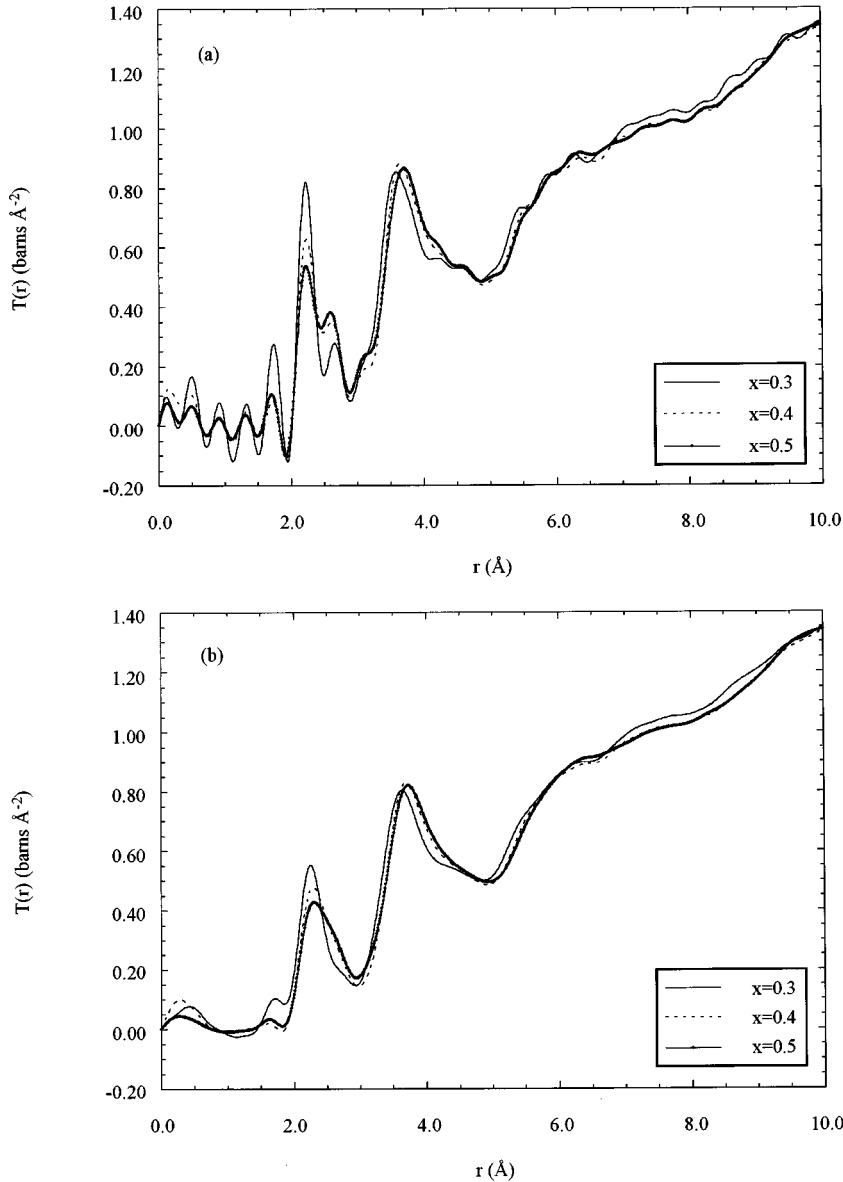


FIG. 3. The total correlation functions $T(r)$ for the glasses of (Ag₂S)_x(GeS₂)_{1-x} obtained by Fourier transforming $i(Q)$ functions using a Q_{\max} of 15.9 \AA^{-1} . (a) No modification function applied; (b) the Lorch function (Ref. 14) applied.

TABLE II. Coordination numbers and bond lengths for $\text{Ag}_2\text{S-GeS}_2$ glasses.

	N_{GeS}	N_{AgS}	$r_{\text{GeS}} (\text{\AA})$	$r_{\text{AgS}} (\text{\AA})$	$r_{\text{AgAg}} (\text{\AA})$	$r_{\text{AgGe}} (\text{\AA})$
$(\text{Ag}_2\text{S})_{0.3}(\text{GeS}_2)_{0.7}$	4.96	3.21	2.23	2.66	3.06	3.58
$(\text{Ag}_2\text{S})_{0.4}(\text{GeS}_2)_{0.6}$	4.97	3.38	2.24	2.63	3.07	3.63
$(\text{Ag}_2\text{S})_{0.5}(\text{GeS}_2)_{0.5}$	5.36	2.85	2.24	2.62	3.06	3.70

and the second peaks at about 1.1 and 2.1 \AA^{-1} , respectively. In particular, it is immediately noted that changes in the first peak, the so-called first sharp diffraction peak (FSDP),⁹ are especially large. It is inferred from the fact that the FSDP is associated with medium-range order (MRO) that the addition of Ag_2S modifies the MRO in the GeS_2 network significantly. It is further observed that, as the concentration of the modifier Ag_2S increases, the intensity of the FSDP decreases: the degree of MRO changes is dependent on the concentration of the added salt. Similar features have been reported previously for a number of other glasses.^{10,11}

The trends in the height of the first peak in $i(Q)$ with composition are depicted in Fig. 2. The height of the FSDP decreases almost linearly with Ag_2S concentration. This behavior of the first peak can be understood by the void model,⁹ which explains the FSDP in terms of the chemical ordering between the clusters forming structural units and the interstitial voids surrounding them. In this picture, the FSDP is a prepeak in the concentration-concentration partial structure factor $S_{\text{CC}}(Q)$ in the Bhatia-Thornton formalism¹² for a packing of clusters and voids:

$$i^{\text{BT}}(Q) = N[\langle b \rangle^2 S_{\text{NN}}(Q) + 2C_1 \langle b \rangle (b_1 - b_2) S_{\text{NC}}(Q) + C_1 C_2 (b_1 - b_2)^2 S_{\text{CC}}(Q)], \quad (4)$$

where N is the total number of species (e.g., clusters and voids), C_1 and C_2 are the concentrations, and b_1 and b_2 are the neutron-scattering lengths of species 1 (e.g., cluster) and 2 (e.g., void). $S_{\text{NN}}(Q)$, $S_{\text{NC}}(Q)$, and $S_{\text{CC}}(Q)$ are number-number, number-concentration, and concentration-concentration partial structure factors, respectively, and $\langle b \rangle$ is the compositionally weighted average scattering length, $\langle b \rangle = \sum x_i b_i$. This model proposes that the incorporation of modifier ions into the network former results in the occupation of the interstitial void sites in the framework.

Further investigation of the behavior of the FSDP has involved the simulation of a model system of stuffed silica¹³ and an equation has been derived to explain the compositional dependence of the FSDP intensity. This was done by separating the third term in Eq. (4) as follows:

$$C_1 C_2 (b_1 - b_2)^2 S_{\text{CC}}(Q) \approx C_1 C_2' (b_1 - b_2')^2 S_{\text{CC}}(Q) + C_1 C_2'' (b_1 - b_2'')^2 S_{\text{CC}}(Q), \quad (5)$$

where C_2' and C_2'' are the concentrations ($C_2 = C_2' + C_2''$), and b_2' and b_2'' are the scattering lengths, of the voids and extrinsic atoms (e.g., Ag ions), respectively. The magnitude of the $S_{\text{CC}}(Q)$ term is controlled by the coefficients $C_1 C_2' (b_1 - b_2')^2$ and $C_1 C_2'' (b_1 - b_2'')^2$, but the terms $(b_1 - b_2')^2$ and $(b_1 - b_2'')^2$ remain constant. Therefore, $C_1 C_2'$ and $C_1 C_2''$ play the significant part. Because the value of C_2'' is small compared with C_2' , the FSDP intensity is more

dependent on C_2' which decreases with increasing C_2'' . It can be expected, therefore, that the more voids that are replaced by extrinsic atoms, the lower is the FSDP intensity. However, the $S_{\text{CC}}(Q)$ term itself may also alter with the modifier concentration in a system such as $\text{Ag}_2\text{S-GeS}_2$. Nevertheless, the dependence of the FSDP height on the Ag_2S composition observed experimentally seems to be linear, with a deviation from linearity beginning at the concentration of $x=0.4$ (Fig. 2). This feature suggests that $S_{\text{CC}}(Q)$ is essentially constant (in the region of the FSDP) for Ag_2S concentrations less than $x=0.4$.

On the other hand, the second peak in $i(Q)$ at about 2.1 \AA^{-1} exhibits the opposite trend of intensity changes to that of the first peak (Fig. 2): the height becomes larger as the concentration of the modifier increases. The cluster-void model proposes that the second peak in the structure factor is the first peak in the number-number structure factor $S_{\text{NN}}(Q)$ in the Bhatia-Thornton formalism.¹² Application of this model to the $\text{Ag}_2\text{S-GeS}_2$ system leads to the suggestion that $S_{\text{NN}}(Q)$ (in the vicinity of the second peak) is an increasing linear function of the Ag_2S composition, with the linearity starting to deviate at a concentration of $x=0.4$ as does that of the first peak height (Fig. 2). Since the value of $\langle b \rangle^2$, the coefficient of $S_{\text{NN}}(Q)$ [Eq. (4)], stays at around a value of 0.22 barns for all modifier concentrations (Table I), this quantity does not act as the intensity controlling factor.

B. $(\text{Ag}_2\text{S})_x(\text{GeS}_2)_{1-x}$ glasses: total correlation function $T(r)$

Each $i(Q)$ data set was Fourier transformed to give $T(r)$ using a Q_{max} of 15.9 \AA^{-1} but using no modification function [Fig. 3(a)]; hence oscillations at low r resulting from the truncation were unavoidable. Among the low- r fluctuations (before a major peak at 2.2 \AA) which are supposed to originate from the truncation effect, a peak at about 1.7 \AA looks intense enough to contain real structural information. In order to suppress the artifacts in the low- r range to see whether this peak may be structurally meaningful, the $i(Q)$ functions were also Fourier transformed to $T(r)$ functions by applying a Lorch modification function¹⁴ [Fig. 3(b)]. As expected, the two peaks at 2.2 and 2.6 \AA merge together and form a broad peak. However, the intensity of the peak at approximately 1.7 \AA still remains considerable. This test indicates that this peak may contain structural meaning and not be simply a termination ripple.

The peak at 1.7 \AA may result from Ge-O correlations. This possibility is based on the results from studies on GeO_2 glass, where the Ge-O bond length has been identified as being 1.72 \AA (Ref. 14) or 1.74 \AA .¹⁵ We believe that oxygen contamination from water, creating Ge-O chemical bonds, is not the primary cause, but that oxygen contamination of the starting Ge material is responsible.

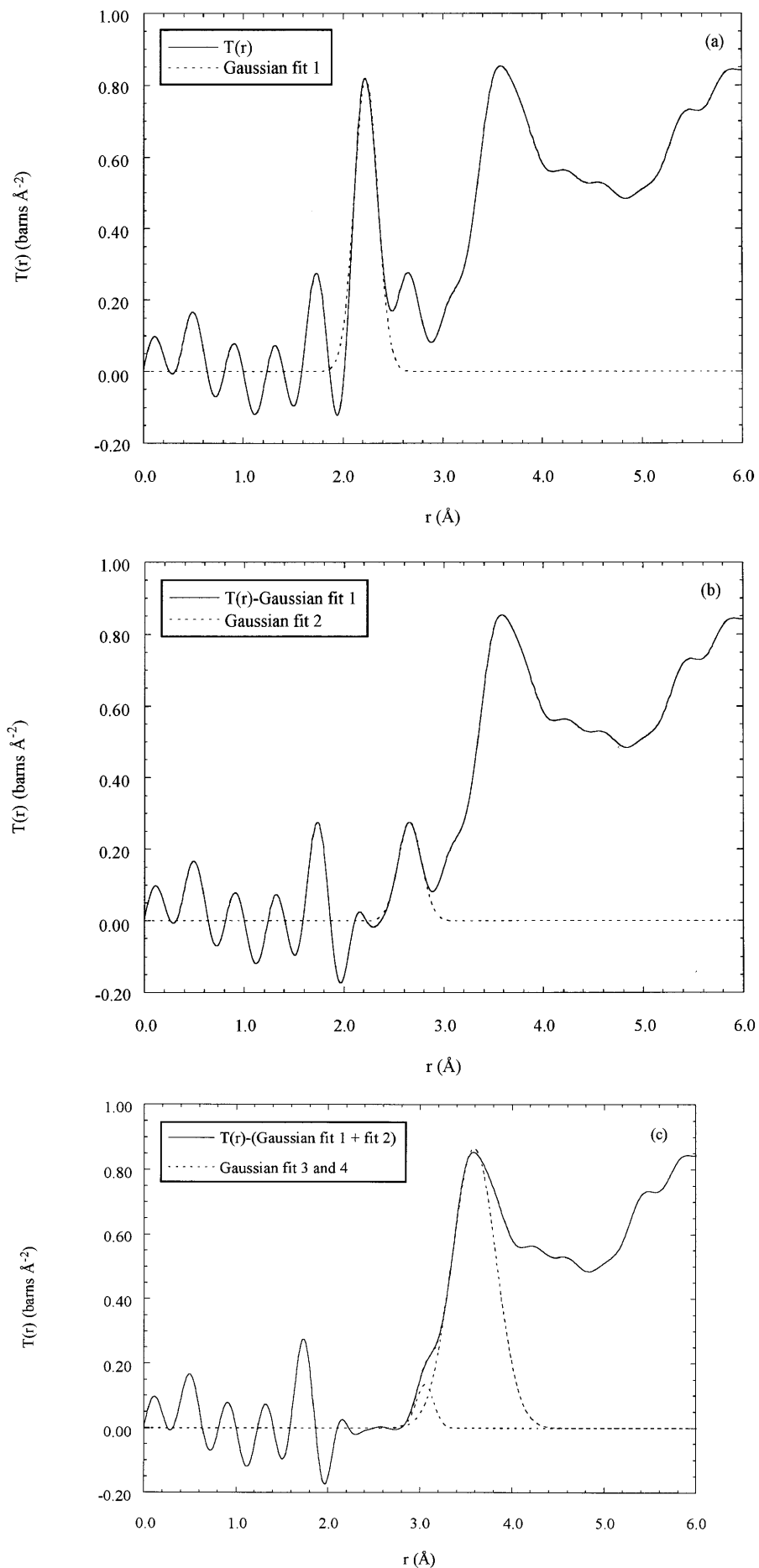


FIG. 4. The Gaussian fitting steps taken to estimate the coordination numbers for the $(\text{Ag}_2\text{S})_{0.3}(\text{GeS}_2)_{0.7}$ glass. (a) A Gaussian function was fitted to the peak at 2.2 \AA . (b) The Gaussian function found was subtracted from $T(r)$ and another Gaussian function fitting to the peak at 2.6 \AA was found. (c) This Gaussian function was also subtracted from the function of [$T(r)$ -first Gaussian function] and a sum of two Gaussian functions were found to fit the broad peak at 3-4 \AA .

The peak at about 2.2 Å is assigned to Ge-S correlations in a GeS₄ coordination polyhedron. This conclusion is based on a number of experimental results. The Ge-S bond length in high- and low-temperature crystalline forms of GeS₂ obtained from x-ray crystallography^{16,17} is 2.217 and 2.224 Å, respectively. The Ge-S bond length has been determined to be 2.23 Å in *g*-GeS₂ from x-ray-diffraction studies.¹⁸ Ge *K*-edge x-ray-absorption spectroscopy results for *g*-GeS₂,^{6,19} gave a Ge-S bond length of 2.22 Å. It was observed in this study that the Ge-S bond length stays nearly constant during the process of adding modifier ions (see Table II). This indicates that this length corresponds to that of covalent Ge-S bonds.

The following peak at about 2.6 Å is identified as an Ag-S correlation. This presumption is supported by an x-ray crystallography study on β-Ag₂S,²⁰ which gave evidence for three types of Ag-S bonds depending on whether Ag ions sit in octahedral or tetrahedral sites surrounded by S: an octahedral site with two types of average Ag-S bond lengths of 2.49 and 3.43 Å, and a tetrahedral site with an average Ag-S bond length of 2.70 Å (three at 2.61 Å and one at 2.99 Å). More directly, Ag *K*-edge x-ray-absorption studies on (Ag₂S)_{*x*}(GeS₂)_{1-*x*} glasses measured at 35 K gave an Ag-S bond length of 2.53–2.54 Å for the compositions of *x*=0.3, 0.4, 0.5.²¹ Unlike the observation that Ge-S bonds remain at about the same length after the addition of the modifier Ag₂S into the GeS₂ framework, it appears that the Ag-S bonds in (Ag₂S)_{*x*}(GeS₂)_{1-*x*} glasses become slightly shorter with increasing Ag₂S content (Table II).

Coordination numbers corresponding to these two assigned correlations (Ge-S and Ag-S) were obtained by fitting each peak to a Gaussian function for which the area was integrated. The Gaussian fitting steps for the (Ag₂S)_{0.3}(GeS₂)_{0.7} sample as an example are depicted in Fig. 4. First, a Gaussian function was fitted to the Ge-S peak at 2.2 Å [Fig. 4(a)] and this function was subtracted from *T*(*r*) [Fig. 4(b)]. Then, another Gaussian function fitting to the Ag-S peak at 2.6 Å was found, again followed by a subtraction from the function of [*T*(*r*)-first Gaussian function]. This procedure was repeated.

The peaks at higher *r* are difficult to fit because they are not well separated. The next peak after the Ag-S correlation, for example, shows a shoulder on its left side [Fig. 4(c)]. This broad peak, in a range of approximately 3–4 Å, was therefore fitted to a sum of two Gaussian functions. This assumes that there are only two correlations contributing to this peak.

The peak at about 3 Å can be assigned to Ag-Ag contributions. This interpretation is based on a crystallographic study of the low-temperature form of synthetic argyrodite Ag₈GeS₆ (Ref. 22) that concluded that all Ag atoms have at least one near-Ag neighbor between 2.93 and 3.11 Å. The following broad peak positioned at about 3.6–3.7 Å is considered to be due to Ag-Ge correlations. This peak identification will be discussed in more detail in Sec. IV D.

Likewise, coordination numbers for the other two samples, (Ag₂S)_{0.4}(GeS₂)_{0.6} and (Ag₂S)_{0.5}(GeS₂)_{0.5}, were also estimated. The goodness of the fits for all three samples are presented in Fig. 5 and the results are summarized in Table II.

It is immediately noted from Table II that the average number of S atoms around Ge in each sample is bigger than the value of four which is generally postulated in the case of network formers based on a tetrahedral structure. It is in fact unlikely that Ge, a tetravalent atoms, has more than four neighboring atoms (covalent bonds). This means the *N*_{GeS} values are probably overestimated in this neutron-diffraction study. Ge *K*-edge EXAFS results for the system (Ag₂S)_{*x*}(GeS₂)_{1-*x*} have in fact provided values less than 4: *N*_{GeS}=3.7, 3.4, and 3.6 for *x*=0.3, 0.4, and 0.5, respectively.⁶ Considering the relatively small value of *Q*_{max} of 15.9 Å used for Fourier transformation in this study, however, overestimations for the first (and the second) peak coordination numbers are unavoidable. The coordination number and bond length estimated from the first peak in *T*(*r*) are dependent on the value of *Q*_{max} used. Unless a sufficiently large value of *Q*_{max} is used, the areas of the first few peaks tend to be larger than those expected and their peak positions may shift slightly depending on the *Q*_{max}.²³ Coordination numbers are also subject to the way in which peaks are fitted by Gaussian functions, and the method that we chose to employ for this study (see Fig. 4) tends to result in overestimates for the coordination of first peaks.²⁴ Nevertheless, any trends in changes of coordination numbers or bond lengths with the Ag₂S concentration (Table II) are meaningful since the same value of *Q*_{max} was used in all three cases.

The compositional dependence of the coordination numbers and bond lengths for the glassy (Ag₂S)_{*x*}(GeS₂)_{1-*x*} system are given in Table II. There seems to be no particular trend in coordination numbers with composition. This is consistent with EXAFS results from Ge and Ag *K*-edge experiments on the same system.^{6,21} The fact that *N*_{Ge-S} and *N*_{Ag-S} do not change linearly according to the Ag₂S concentration leads to the conclusion that the structure of the intermediate glass composition (Ag₂S)_{0.4}(GeS₂)_{0.6} does not necessarily possess a structure intermediate between those of the other two compositions, (Ag₂S)_{0.3}(GeS₂)_{0.7} and (Ag₂S)_{0.5}(GeS₂)_{0.5}.

Unlike the coordination numbers, the bond lengths do exhibit some systematic trends (Table II): the first three peak positions stay more or less the same, while the fourth peak position gradually shifts to higher values as the concentration of the modifier increases.

C. Isotopically substituted (Ag₂S)_{0.5}(GeS₂)_{0.5} glasses: distinct scattering function *i*(*Q*)

The *i*(*Q*) functions for the three different isotopically substituted samples of the glass system (Ag₂S)_{0.5}(GeS₂)_{0.5} are shown in Fig. 6. The curves are similar to each other, particularly at large *Q* values, but major differences are found in the first and second peaks, at about 1.1 and 2.1 Å⁻¹, respectively. Moreover, the changes in intensity of these first two peaks are observed to be systematically related to the scattering length of the Ag isotope involved: the height of the first peak decreases, whereas that of the second peak increases, as a linear function of the scattering length of the Ag isotope (Fig. 7).

As described in Sec. IV A, such changes in the intensity of the first and the second peaks can be understood in terms of the void model.¹³ Given the same structure but with dif-

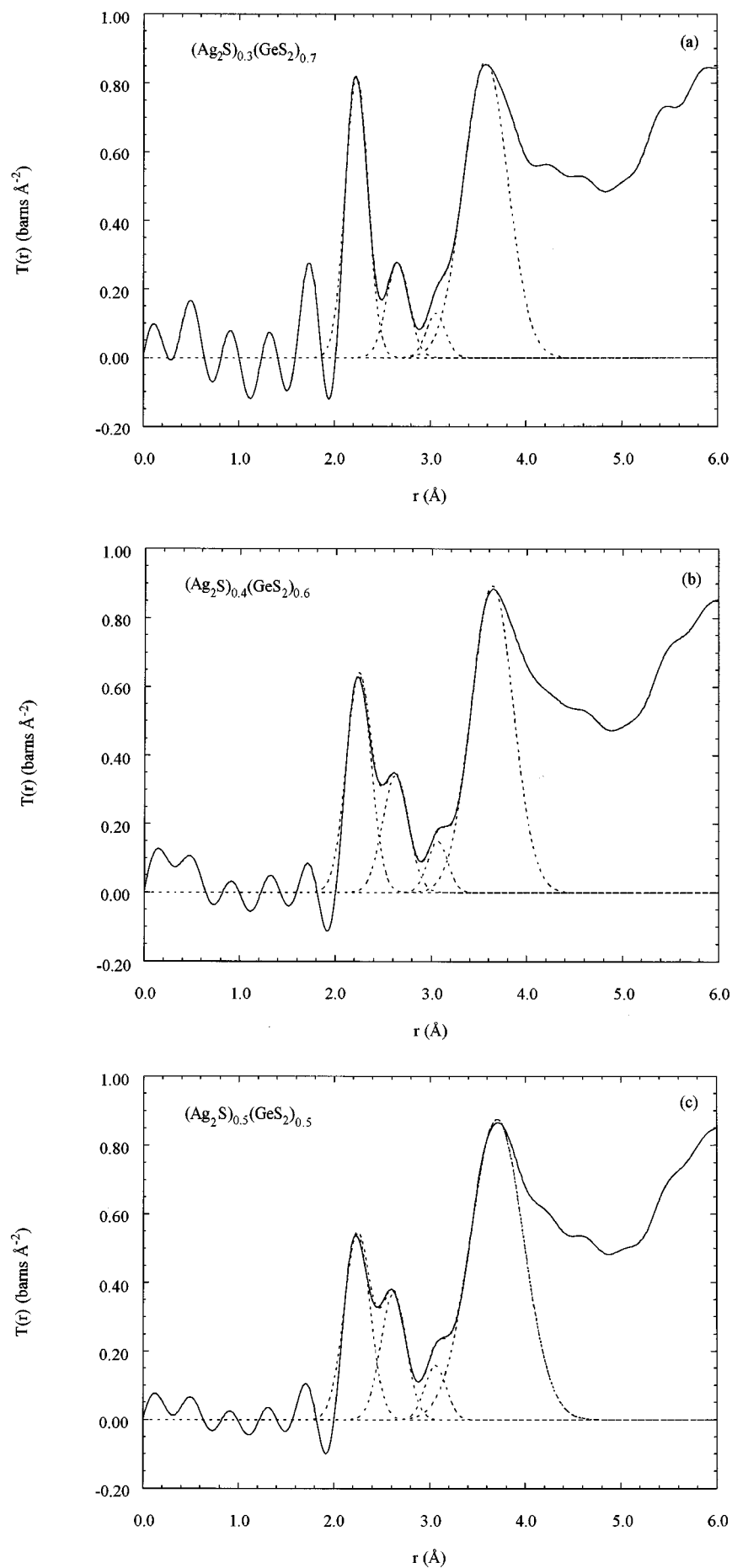


FIG. 5. The Gaussian fitting results for the three samples. (a) $(\text{Ag}_2\text{S})_{0.3}(\text{GeS}_2)_{0.7}$, (b) $(\text{Ag}_2\text{S})_{0.4}(\text{GeS}_2)_{0.6}$, and (c) $(\text{Ag}_2\text{S})_{0.5}(\text{GeS}_2)_{0.5}$.

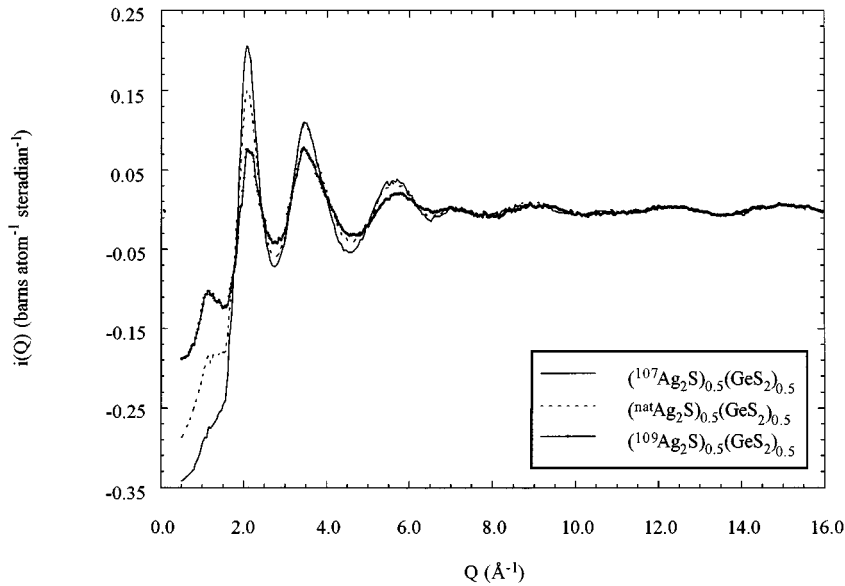


FIG. 6. The $i(Q)$ functions for the three different isotopically substituted samples of the glass system $(\text{Ag}_2\text{S})_{0.5}(\text{GeS}_2)_{0.5}$.

ferent isotopes, C_2' and C_2'' remain constant and the first term in Eq. (5) is unchanged with the isotopic variation. Therefore, the only term crucially controlling $S_{\text{CC}}(Q)$ is that involving the scattering length of Ag isotopes $(b_1 - b_2)''^2$, which can be represented as $(b_{\text{Ge}} - b_{\text{Ag}})''^2$. The term controlling the intensity of the second peak [i.e., $S_{\text{NN}}(Q)$] is merely $\langle b \rangle^2$. Figure 7 shows for comparison the values of these coefficients on which, for the void model, the first and the second peak intensities are dependent. It is manifest that the void model can interpret the behavior of the first and second peaks in $i(Q)$ observed experimentally for the isotopically substituted $(\text{Ag}_2\text{S})_{0.5}(\text{GeS}_2)_{0.5}$ glass.

D. Isotopically substituted $(\text{Ag}_2\text{S})_{0.5}(\text{GeS}_2)_{0.5}$ glasses: total correlation function $T(r)$

$T(r)$ functions were obtained by Fourier transforming $i(Q)$ functions using a Lorch modification function¹⁴ with a Q_{max} of 27.8 \AA^{-1} (Fig. 8). It should be mentioned that these

$T(r)$ functions are not completely identical to those presented in the previous paper,⁷ where no modification function with a smaller Q_{max} of 18.4 \AA^{-1} was used. Truncation effects were reduced immensely by applying the Lorch function, in comparison with the results from D4b (Fig. 3). Figure 9(a) shows the $i(Q)$ functions for the $(\text{Ag}_2\text{S})_{0.5}(\text{GeS}_2)_{0.5}$ glass measured by the two different neutron diffractometers. The D4b data extend over a range of less than 16 \AA^{-1} whereas the LAD data extend for over 30 \AA^{-1} . Apart from this difference in the available Q range, the two $i(Q)$ functions are nearly the same.

The total radial distribution functions obtained by Fourier transformation of the data shown in Fig. 9(a) are compared in Fig. 9(b). As well as differences in the degree of the truncation effects, there are a couple of discrepancies noted between these two functions. These differences are based on variations in the way the Fourier transformation was carried out, namely how large a Q_{max} was used and whether or not a modification function was applied. First, an appreciable dif-

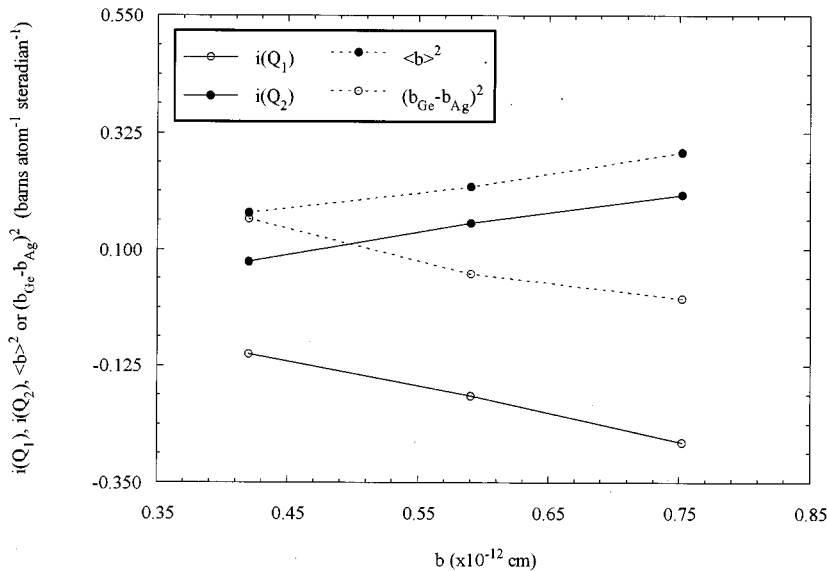


FIG. 7. The variation of the height of the first and second peaks in $i(Q)$, $i(Q_1)$, and $i(Q_2)$, respectively, together with values of $\langle b \rangle^2$ and $(b_{\text{Ge}} - b_{\text{Ag}})''^2$, with the scattering length of silver.

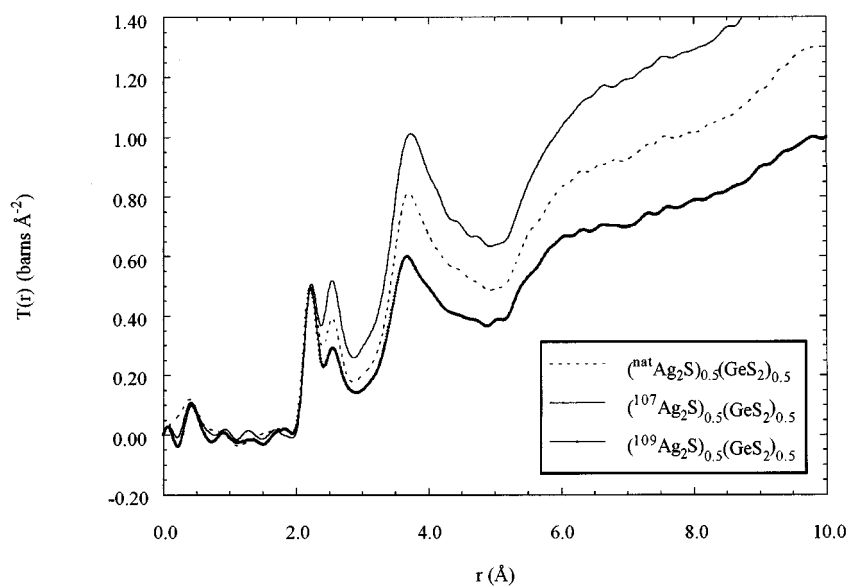


FIG. 8. $T(r)$ functions of different isotopically substituted compounds obtained by Fourier transforming $i(Q)$ using a Lorch modification function (Ref. 14) with a Q_{\max} of 27.8 \AA^{-1} .

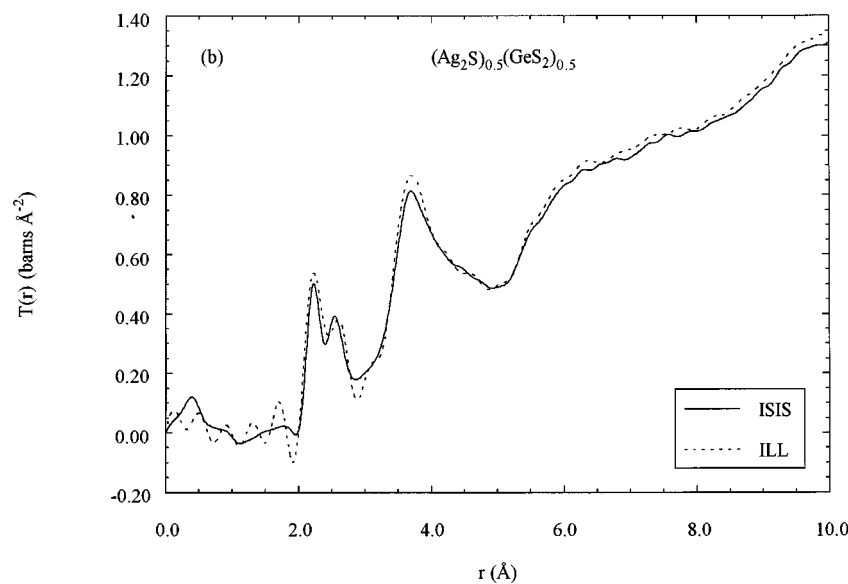
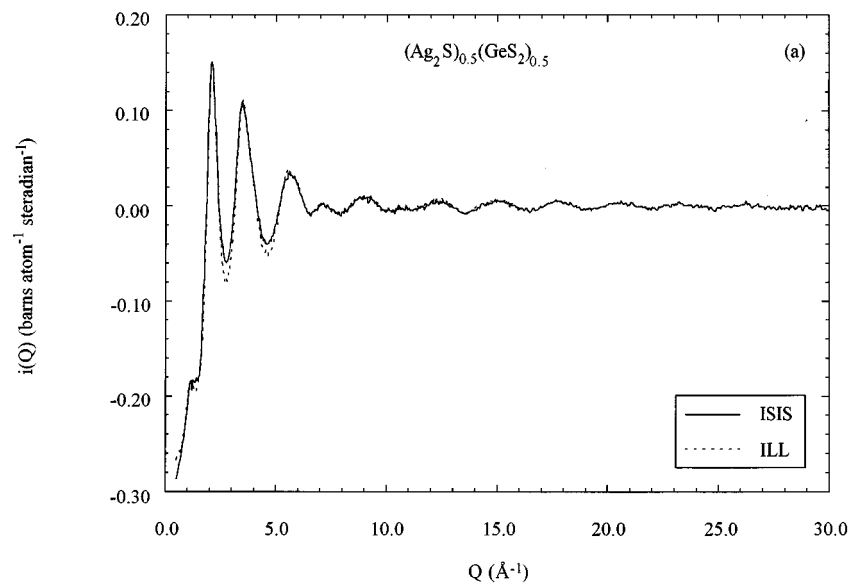


FIG. 9. A comparison of (a) $i(Q)$ and (b) $T(r)$ functions of the $(\text{Ag}_2\text{S})_{0.5}(\text{GeS}_2)_{0.5}$ glass obtained from the two different neutron diffractometers.

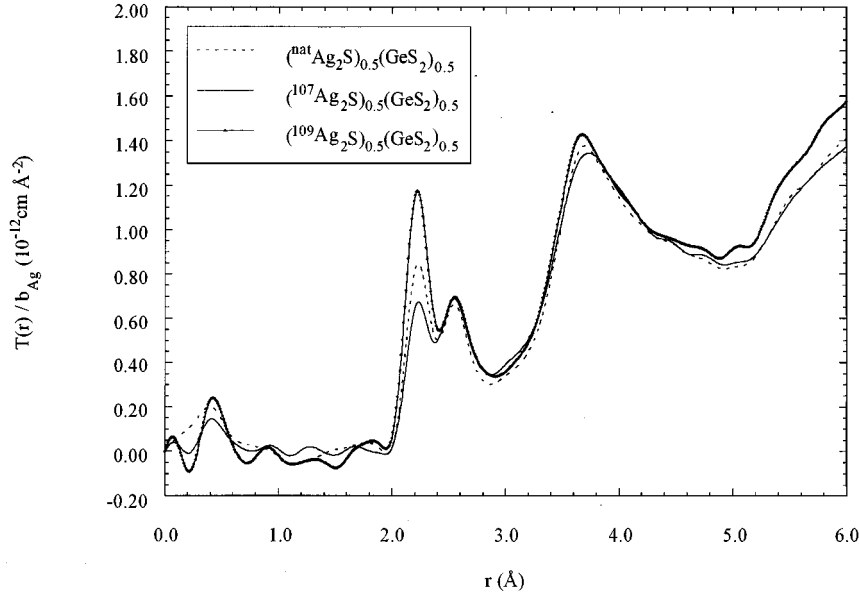


FIG. 10. The function $T(r)/b_{\text{Ag}}$ obtained for each isotopically substituted compound.

ference is noted in the second peak positions in $T(r)$: 2.62 and 2.55 Å from D4b and LAD, respectively. If a too low value of Q_{max} is used for Fourier transformation, the short-range correlations tend to shift slightly from the expected positions.¹⁴ Secondly, the magnitude of $T(r)$ at high r is not quite the same in each case because compositional differences resulted in a slightly different value of T_0 for each function.

It is significant that the area of the first peak is the same in each isotopically substituted sample (Fig. 8). Having identified that the first peak at 2.2 Å is due to the Ge-S correlation alone (no Ag contribution to this peak), $T(r)$ in the range of 2.0–2.3 Å may be rewritten as $T(r) \approx 2x_{\text{Ge}}x_{\text{S}}b_{\text{Ge}}b_{\text{S}}T_{\text{GeS}}(r)$ and it is therefore seen the area of this peak will not vary with Ag isotopic substitution. Furthermore, under the assumption that the second peak at about 2.6 Å is due solely to Ag-S contributions, the function $T(r)/b_{\text{Ag}}$ is expected to have the same second peak area for all isotopic compositions: $T(r)/b_{\text{Ag}} \approx x_{\text{Ag}}x_{\text{S}}b_{\text{S}}T_{\text{AgS}}(r)$. Examination of the heights of the second peak for data plotted in this way (Fig. 10) shows that this peak identification is plausible. Table III gives the scattering lengths of the three Ag isotopes used in this study.

As described previously,⁷ the first and second differences in $D(r)$ functions from two different isotopically substituted samples can be calculated. The first difference $\Delta D(r)$ can be written as follows:

$$\Delta D(r) = D(r) - D^*(r) = AG_{\text{SAg}}(r) + BG_{\text{GeAg}}(r)$$

$$+ CG_{\text{AgAg}}(r), \quad (6)$$

where $A = 2x_{\text{S}}x_{\text{Ag}}b_{\text{S}}(b_{\text{Ag}} - b_{\text{Ag}}^*)$, $B = 2x_{\text{Ge}}x_{\text{Ag}}b_{\text{Ge}}(b_{\text{Ag}} - b_{\text{Ag}}^*)$ and $C = x_{\text{Ag}}^2(b_{\text{Ag}}^2 - b_{\text{Ag}}^{*2})$. The asterisk is to distinguish different isotopic species. Table IV summarizes the values of A , B , and C for each pair of isotopic samples. The significance of the $\Delta D(r)$ function in this case is that it is a sum of the three partial correlation functions involving Ag.

Given the three $\Delta D(r)$ functions, the partial correlation function $G_{\text{AgAg}}(r)$ can be obtained via matrix inversion.⁷ Having calculated $G_{\text{AgAg}}(r)$, it is also possible to rearrange the $D(r)$ functions and obtain a weighted sum of the two partial correlation functions $G_{\text{SAg}}(r)$ and $G_{\text{GeAg}}(r)$:

$$\begin{aligned} & x_{\text{S}}b_{\text{S}}G_{\text{SAg}}(r) + x_{\text{Ge}}b_{\text{Ge}}G_{\text{GeAg}}(r) \\ &= \frac{\Delta D(r) - x_{\text{Ag}}^2(b_{\text{Ag}}^2 - b_{\text{Ag}}^{*2})G_{\text{AgAg}}(r)}{2x_{\text{Ag}}(b_{\text{Ag}} - b_{\text{Ag}}^*)}. \end{aligned} \quad (7)$$

These functions [Eq. (7)] from three pairs of different isotopically substituted samples are depicted in Fig. 11. Neglecting fluctuations arising from artifacts of the first and second differences calculations in the region of r less than 2.0 Å, where no physically meaningful correlations are expected, there are two features to be noted: one peak lying at about 2.6 Å which has already been assigned to Ag-S correlations and another present at about 3.7 Å. The function on the right-hand side of Eq. (7) is a weighted sum of Ag-S and Ag-Ge correlations alone. Given the identification of the peak at 2.6 Å as being explicitly due to Ag-S contributions,

TABLE III. Scattering lengths and isotopic enrichments of the three different Ag isotopes used in this study.

	Isotopic ratio	Scattering length b (cm^{-12})
¹⁰⁷ Ag enriched	99% ¹⁰⁷ Ag + 1% ¹⁰⁹ Ag	0.7521
^{nat} Ag	51.83% ¹⁰⁷ Ag + 48.17% ¹⁰⁹ Ag	0.5922
¹⁰⁹ Ag enriched	1% ¹⁰⁷ Ag + 99% ¹⁰⁹ Ag	0.4199

TABLE IV. Values of A , B , and C for each pair of isotopic samples: $A = 2x_S x_{Ag} b_S (b_{Ag} - b_{Ag}^*)$, $B = 2x_{Ge} x_{Ag} b_{Ge} (b_{Ag} - b_{Ag}^*)$, and $C = x_{Ag}^2 (b_{Ag}^2 - b_{Ag}^{*2})$.

	A (barns)	B (barns)	C (barns)
^{107}Ag enriched vs $^{\text{nat}}\text{Ag}$ sample	0.0153	0.0147	0.0241
$^{\text{nat}}\text{Ag}$ vs ^{109}Ag -enriched sample	0.0162	0.0155	0.0191
^{107}Ag vs ^{109}Ag -enriched sample	0.0315	0.0302	0.0433

the peak at 3.7 Å can consequently be identified as due to Ag-Ge correlations. A very similar result has been obtained from anomalous wide angle x-ray-scattering studies on the glass $(\text{Ag}_2\text{S})_{0.5}(\text{GeS}_2)_{0.5}$, namely an Ag-Ge bond length of 3.8 Å.²⁵

A weighted sum of the three partial correlation functions which do not include Ag contributions can also be obtained by rearranging the $\Delta D(r)$ functions and $G_{\text{AgAg}}(r)$.⁷ This sum is

$$\begin{aligned} \Delta D'(r) &= \frac{D(r) - (b_{\text{Ag}}/b_{\text{Ag}}^*)D^*(r)}{1 - b_{\text{Ag}}/b_{\text{Ag}}^*} + x_{\text{Ag}}^2 b_{\text{Ag}} b_{\text{Ag}}^* G_{\text{AgAg}}(r) \\ &= x_S^2 b_S^2 G_{\text{SS}}(r) + 2x_S x_{\text{Ge}} b_S b_{\text{Ge}} G_{\text{SGe}}(r) \\ &\quad + x_{\text{Ge}}^2 b_{\text{Ge}}^2 G_{\text{GeGe}}(r) \end{aligned} \quad (8)$$

and is plotted in Fig. 12. As well as the first peak at 2.2 Å which is identified as being due to Ge-S correlations, there are two additional major peaks in the low- r region, say less than 4 Å: one at about 2.7 Å and the other at about 3.4 Å. Since Ge K -edge EXAFS studies of the GeS_2 glass provide an estimate for the corner-sharing Ge-Ge distance of 3.44 Å,¹⁹ the peak at 3.4 Å is ascribed to such Ge-Ge contributions. So far, two out of three peaks noted have been identified to be due to S-Ge and Ge-Ge correlations. Because the function $\Delta D'(r)$ is a sum of three partial correlations S-S, S-Ge, and Ge-Ge, the peak at 2.7 Å is most likely due to S-S correlations. It seems that this length is rather short as an S-S contribution. For example, the average S-S bond length is

3.408 Å in edge-sharing GeS_4 tetrahedra in the structure of the low-temperature crystalline form of GeS_2 .¹⁷

The purpose of the calculation involving Eq. (8) is to extract as much information as possible out of data obtained from a set of three isotopically substituted samples but success depends absolutely on the quality of the data. It is noted that, although in theory the three $\Delta D'(r)$ functions should be the same as there is no Ag contribution to these functions, there is some discrepancy between $\Delta D'(r)$ functions calculated from different pairs of isotopically substituted samples (Fig. 12). The cause of this discrepancy lies almost solely in the multisubtraction process involved in calculating Eq. (8). By assuming slightly different chemical compositions in the calculation of $G_{\text{AgAg}}(r)$, it was found that slight compositional deviations, for example $\text{Ag}_{0.333}\text{Ge}_{0.157}\text{S}_{0.510}$ which is the experimentally determined composition of the natural sample, from the stoichiometry $(\text{Ag}_2\text{S})_{0.5}(\text{GeS}_2)_{0.5}$ make no significant contribution to this discrepancy. It could be then argued that the peak at 2.7 Å may well be an artifact from the multisubtraction process. However, the GeS_4 tetrahedra do not necessarily remain regular after the addition of a modifier in an amount of half the molar ratio of the network former itself. We suggest later in this section a slightly elongated tetrahedron model, involving short S-S distances, for the short-range order in this modified glass.

The Ag-Ag correlation function $G_{\text{AgAg}}(r)$ is shown in Fig. 13 together with $D(r)$ for the natural sample for comparison. Although the $G_{\text{AgAg}}(r)$ function is noisy, a very broad contribution of Ag-Ag correlations is observed in the region of 2.5–3.5 Å, in agreement with the correlation at

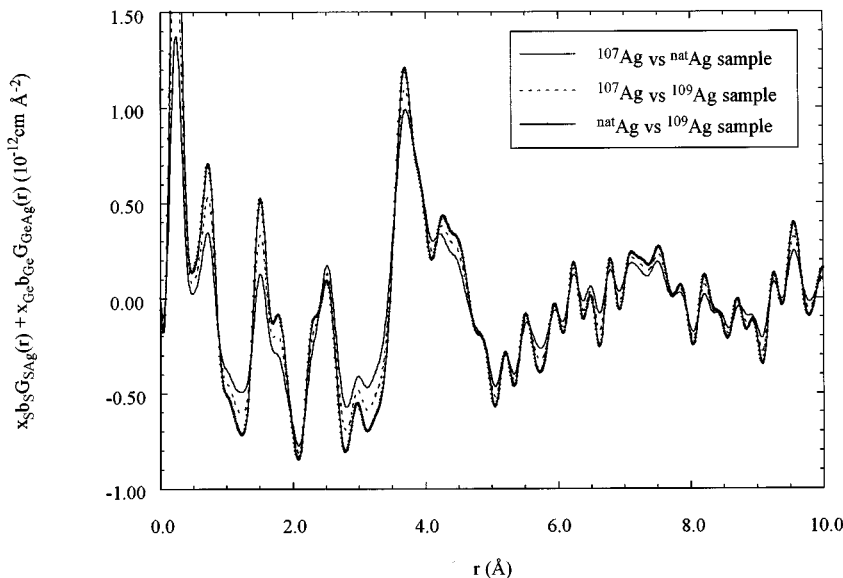


FIG. 11. The function $x_S b_S G_{\text{S}_{\text{Ag}}}(r) + x_{\text{Ge}} b_{\text{Ge}} G_{\text{Ge}_{\text{Ag}}}(r)$ from each pair of different isotopically substituted samples.

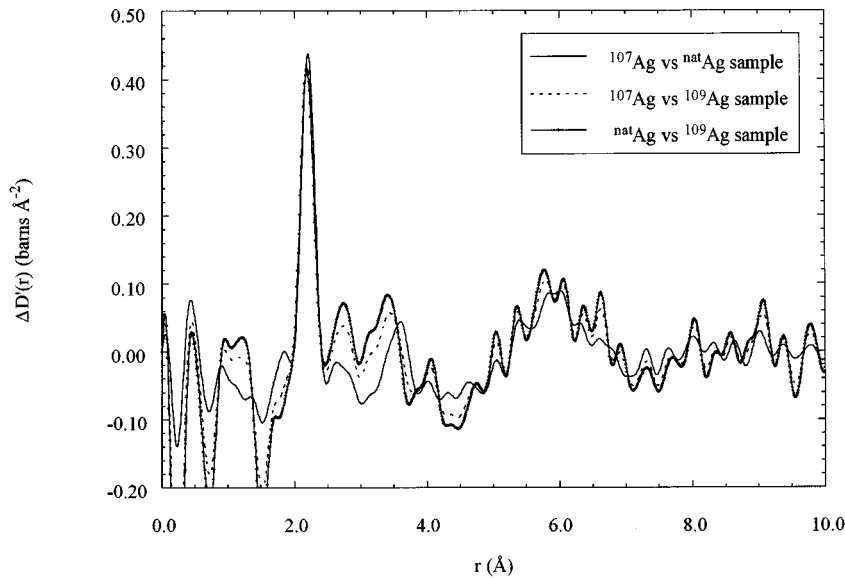


FIG. 12. The function $\Delta D'(r)$ from each pair of different isotopically substituted samples.

approximately 3 Å found by Gaussian fitting of peaks in $T(r)$ [Fig. 5(c) and Table II], and with the results of a previous reverse Monte Carlo simulation.⁷

Each peak in $T(r)$ for the isotopically substituted samples was fitted to a Gaussian function in the same way as described in Sec. IV A in order to estimate the coordination numbers. The goodness of the fit is shown in Fig. 14 and the coordination numbers and bond lengths obtained are summarized in Table V. It is seen that the coordination numbers and the bond lengths differ very slightly from one sample to another, possibly owing to compositional variations. Nevertheless, these deviations are deemed insignificant.

The number of S atoms around a Ge atom, N_{GeS} , was determined to be approximately 3.7, which is slightly smaller than the value four characteristic of tetrahedral coordination. The structural parameters deduced from the fit to the first peak are in good agreement with results from extended x-ray-absorption fine structure (EXAFS) experiments on the

same system.⁶ EXAFS measurements at the Ge K edge at room temperature have provided values of 2.22 Å for the Ge-S bond length and 3.6 for N_{GeS} .⁶

From Ag K -edge EXAFS results measured at 290 K,²¹ the Ag-S bond length was obtained to be 2.5 Å which is supportive of the peak identification of this study: the peak at 2.6 Å is due to Ag-S correlations. Moreover, the average of the three N_{AgS} values found in this study is 2.89, being nearly the same as the value 2.9 obtained from the same EXAFS study.²¹ This argument can be further assured by comparing it with crystallographic results from Ag_8GeS_6 .²² There are three types of Ag positions in relation to S: strongly distorted tetrahedra, approximately planar threefold coordination and almost linear coordination by two S atoms. The corresponding Ag-S distances are 2.56–2.94, 2.49–2.76, and 2.42–2.44, respectively. Having obtained the result that the Ag-S bond length is 2.6 Å with a coordination number 2.9, it can be inferred that the local structural environment of

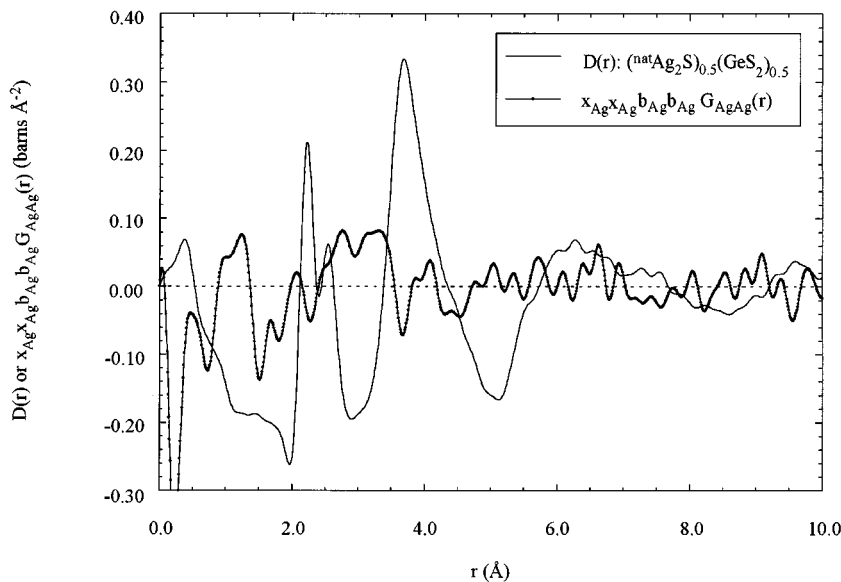


FIG. 13. The weighted function $G_{\text{AgAg}}(r)$, together with $D(r)$ for the natural isotope sample $(\text{natAg}_2\text{S})_{0.5}(\text{GeS}_2)_{0.5}$ for comparison.

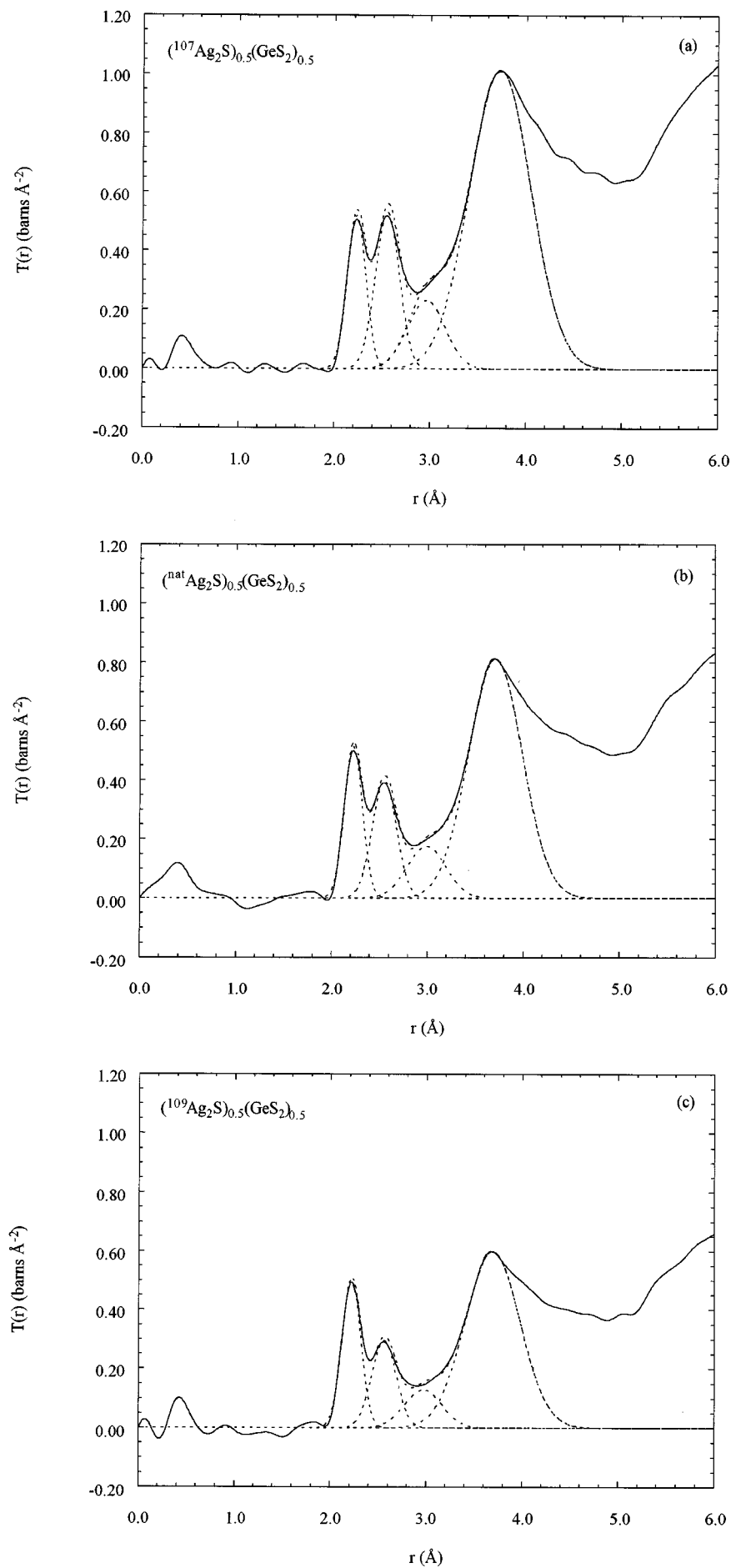


FIG. 14. The Gaussian fitting results for the three isotopically substituted samples. (a) $(^{107}\text{Ag}_2\text{S})_{0.5}(\text{GeS}_2)_{0.5}$, (b) $(^{\text{nat}}\text{Ag}_2\text{S})_{0.5}(\text{GeS}_2)_{0.5}$, and (c) $(^{109}\text{Ag}_2\text{S})_{0.5}(\text{GeS}_2)_{0.5}$.

TABLE V. Bond lengths and coordination numbers of the isotopically substituted $(\text{Ag}_2\text{S})_{0.5}(\text{GeS}_2)_{0.5}$ glass.

	N_{GeS}	N_{AgS}	r_{GeS} (Å)	r_{AgS} (Å)	r_{AgAg} (Å)	r_{AgGe} (Å)
$(^{107}\text{Ag}_2\text{S})_{0.5}(\text{GeS}_2)_{0.5}$	3.73	2.79	2.23	2.55	2.96	3.73
$(^{\text{nat}}\text{Ag}_2\text{S})_{0.5}(\text{GeS}_2)_{0.5}$	3.72	2.87	2.23	2.55	2.99	3.71
$(^{109}\text{Ag}_2\text{S})_{0.5}(\text{GeS}_2)_{0.5}$	3.75	3.01	2.22	2.56	2.97	3.69
Average	3.73	2.89	2.23	2.55	2.97	3.71

Ag in glassy $(\text{Ag}_2\text{S})_{0.5}(\text{GeS}_2)_{0.5}$ greatly resembles the threefold-coordinated local structure of Ag in crystalline Ag_8GeS_6 .

Given the bond lengths of Ge-S and S-S, 2.2 and 2.7 Å, respectively, the associated average S-Ge-S angle is calculated to be approximately 75.7° . Knowing that Ge atoms form a tetrahedral structure with S atoms, the magnitude of this angle appears considerably smaller than the value 109.5° for a regular tetrahedron. This observation, together with the estimated coordination numbers of $N_{\text{GeS}}=3.73$ and $N_{\text{AgS}}=2.89$, leads to a model for the coordination polyhedra and their connection in this system. The model we suggest for the local structure is a deformed tetrahedron whose faces consist of three isosceles triangles and one equilateral triangle (Fig. 15). Four S atoms occupy the four corners of this

tetrahedron and a Ge atom sits in the center of it. Two of these four S atoms surrounding a Ge, leading to a chainlike structure of linked GeS_4 tetrahedra, are nonbridging. A silver atom sits in an interstitial site where it is coordinated by three nonbridging S atoms from three neighboring tetrahedra. Furthermore, this configuration is consistent with other observations: the Ge-Ag bond length of 3.7 Å and the Ag-Ag bond length of 3.0 Å (Fig. 15). We suppose that the three S-S distances greater than 2.7 Å in the elongated tetrahedral unit (Fig. 15) cannot be distinguished in the difference function $\Delta D'(r)$ (Fig. 12).

It is interesting to note that the picture of the static atomic structure of glassy $(\text{Ag}_2\text{S})_{0.5}(\text{GeS}_2)_{0.5}$ that emerges from this neutron-diffraction study is one of a chainlike structure of corner-linked GeS_4 tetrahedra (Fig. 15). It is tempting to speculate that the very high Ag^+ ionic conductivity exhibited by this material, associated with a low value of the activation barrier for ionic transport, is the result of the locally one-dimensional (1D) nature of the medium-range order of the host framework. Ag^+ ions are then constrained to move along 1D channels bordered by nonbridging S anions (Fig. 15) for which the activation energy of ionic mobility will be low. Although this picture of the conduction path for Ag^+ ions in glassy $(\text{Ag}_2\text{S})_{0.5}(\text{GeS}_2)_{0.5}$ is consistent with the static structure found in this study, the present neutron-scattering results cannot be used to prove that this is the actual conduction path.

V. CONCLUSIONS

It has been demonstrated that isotopic-substitution neutron diffraction is a technique enabling the investigation of the short-range ordering involving mobile ions in superionic glasses. By studying three samples of isotopically substituted Ag, it was possible to determine the local environment around Ge atoms and Ag ions in the superionic glass $(\text{Ag}_2\text{S})_{0.5}(\text{GeS}_2)_{0.5}$. This study suggests a deformed GeS_4 tetrahedron, with threefold coordination by S of Ag in interstitial positions, as a model for the short-range order in this system, with a chainlike configuration of linked corner-sharing GeS_4 tetrahedra comprising the medium-range order. The high Ag^+ ion conductivity exhibited by this system is probably associated with the conduction path being quasi-one dimensional, along channels bordered by nonbridging S anions and defined by the chainlike medium-range order of the host framework.

Systematic changes observed in the first sharp diffraction peak and the second peak in the measured distinct scattering functions $i(Q)$ with composition and also with Ag isotopic substitution have been explained by the void model.⁹ The experimental trends are in quantitative agreement with those predicted by the void model.

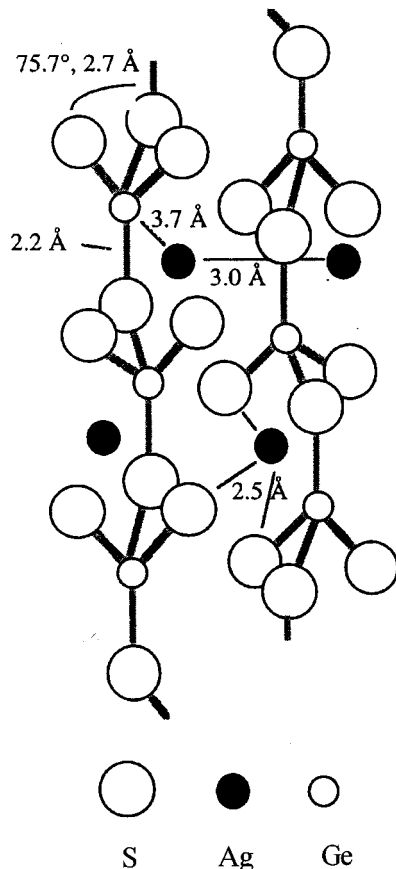


FIG. 15. The coordination polyhedra suggested for the short-range order in the $(\text{Ag}_2\text{S})_{0.5}(\text{GeS}_2)_{0.5}$ glass system: a deformed GeS_4 tetrahedron with threefold coordination by S of Ag ions in interstitial positions.

- ¹E. Robinel, B. Carette, and M. Ribes, *J. Non-Cryst. Solids* **57**, 49 (1983).
- ²J. L. Souquet, E. Robinel, B. Garrau, and M. Ribes, *Solid State Ionics* **3-4**, 317 (1981).
- ³E. Robinel, A. Kone, M. J. Duclot, and J. L. Souquet, *J. Non-Cryst. Solids* **57**, 59 (1983).
- ⁴M. D. Ingram, *Phys. Chem. Glasses* **28**, 215 (1987).
- ⁵J. E. Enderby and G. W. Neilson, *Rep. Prog. Phys.* **44**, 593 (1981).
- ⁶A. Ibanez, E. Philippot, S. Benazeth, and H. Dexpert, *J. Non-Cryst. Solids* **127**, 25 (1991).
- ⁷J. H. Lee, A. P. Owens, A. Pradel, A. C. Hannon, M. Ribes, and S. R. Elliott, *J. Non-Cryst. Solids* **192&193**, 57 (1995).
- ⁸C. N. J. Wagner, M. S. Boldrick, D. Lee, J. Heo, and J. D. Mackenzie, *J. Non-Cryst. Solids* **106**, 50 (1988).
- ⁹S. R. Elliott, *J. Phys. Condens. Matter* **4**, 7661 (1992).
- ¹⁰M. Misawa, D. L. Price, and K. Suzuki, *J. Non-Cryst. Solids* **37**, 85 (1980).
- ¹¹R. J. Dejus, S. Susman, K. J. Volin, D. G. Montague, and D. L. Price, *J. Non-Cryst. Solids* **143**, 162 (1992).
- ¹²A. B. Bhatia and D.E. Thornton, *Phys. Rev. B* **2**, 3004 (1970).
- ¹³J. H. Lee and S. R. Elliott, *Phys. Rev. B* **50**, 5981 (1994); *J. Non-Cryst. Solids* **192&193**, 133 (1995).
- ¹⁴E. Lorch, *J. Phys. C* **2**, 229 (1969).
- ¹⁵J. A. E. Desa and A. C. Wright, *J. Non-Cryst. Solids* **99**, 276 (1988).
- ¹⁶G. Dittmar and H. Schäfer, *Acta Crystallogr. B* **31**, 2060 (1975).
- ¹⁷G. Dittmar and H. Schäfer, *Acta Crystallogr. B* **32**, 1188 (1976).
- ¹⁸A. Feltz, M. Pohle, H. Steil, and G. Herms, *J. Non-Cryst. Solids* **69**, 271 (1985).
- ¹⁹P. Armand, A. Ibanez, H. Dexpert, and E. Philippot, *J. Non-Cryst. Solids* **139**, 137 (1992).
- ²⁰R. M. Cava, F. Reidinger, and B. J. Wuensch, *J. Solid State Chem.* **31**, 69 (1980).
- ²¹A. Ibanez, P. Armand, and E. Philippot, *Solid State Ionics* **59**, 157 (1993).
- ²²G. Eulenberger, *Monatsh. Chem.* **108**, 901 (1977).
- ²³K. Suzuki, in *Methods of Experimental Physics: Neutron Scattering, Part B*, edited by D. L. Price and K. Sköld (Academic, London, 1987).
- ²⁴J. H. Lee, A. C. Hannon, and S. R. Elliott (unpublished).
- ²⁵P. Armand, A. Ibanez, J. M. Tonnerre, D. Raoux, B. Bouchet-Fabre, and E. Philippot, *J. Non-Cryst. Solids* **192&193**, 330 (1995).